BIOCHEMISTRY
including biophysical chemistry & molecular biology

ARTICLE

pubs.acs.org/biochemistry

Impact of p62/SQSTM1 UBA Domain Mutations Linked to Paget's Disease of Bone on Ubiquitin Recognition

Thomas P. Garner,[†] Jed Long,[†] Robert Layfield,[‡] and Mark S. Searle*[,†]

[†]Centre for Biomolecular Sciences, School of Chemistry, University Park, University of Nottingham, Nottingham NG7 2RD, U.K.
[‡]School of Biomedical Sciences, Queen's Medical Centre, University of Nottingham, Nottingham NG7 2UH, U.K.

ABSTRACT: The scaffold protein p62/SQSTM1 acts as a hub in regulating a diverse range of signaling pathways which are dependent upon a functional ubiquitin-binding C-terminal UBA domain. Mutations linked to Paget's disease of bone (PDB) commonly cluster within the UBA domain. The p62 UBA domain is unique in forming a highly stable dimer which regulates ubiquitin recognition by using overlapping surface patches in both dimerization and ubiquitin binding, making the two association events competitive. NMR structural analysis and biophysical methods show that some PDB mutations modulated the ubiquitin binding affinity by both direct and indirect mechanisms that affect UBA structural integrity, dimer stability, and contacts at the UBA−ubiquitin interface. In other cases, common PDB mutations (P392L in particular) result in no significant change in ubiquitin binding affinity for the UBA domain in isolation; however, all PDB UBA mutations lead to loss of function with respect to ubiquitin binding in the context of full-length p62, suggesting a more complex underlying mechanism.

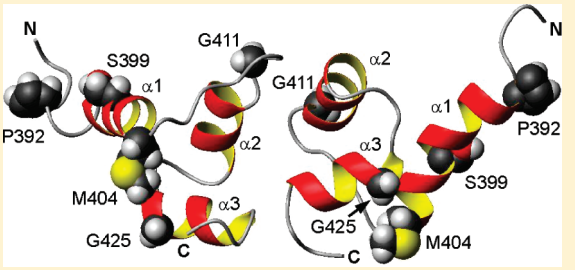

Mutations affecting the p62/SQSTM1 protein are linked to the skeletal disorder Paget's disease of bone (PDB) and commonly, although not exclusively, cluster within the domain boundaries of the C-terminal ubiquitin (Ub) associated (UBA) domain involved in Ub recognition.[1−8] The precise functional implications of the p62 mutations remain unclear although p62 acts as a hub in regulating a diverse range of signaling pathways, including those which lead to activation of the NF-κB family of transcription factors, in part achieved by influencing TRAF6 polyubiquitination.[9−15] Mutations within the UBA domain of p62 appear to represent loss of function with respect to Ub-binding of the full length protein. This may result in the dysregulation of TRAF6 ubiquitination and downstream NF-κB signaling, which with respect to PDB etiology is thought to impact on osteoclastogenesis and osteoclast activity.[3,7] The p62 protein has also been shown to be a shuttle protein for proteasomal degradation[16−18] as well as a key regulator of macroautophagy,[19,20] whereby ubiquitinated protein aggregates, complexes, and organelles are removed from the cell through autophagosomal degradation.

The family of Ub-binding domains (UBDs) found within Ub receptors such as p62 has grown to >20, typically consisting of small motifs of <50 residues.[21] The majority of these bind as monomers with evidence for different polyubiquitin (polyUb) chain specificities in some cases.[22−28] However, the CUE domain of Vps9p and the UBA domain of Cbl-b have been shown to form biologically important dimeric structures which enhance Ub-binding.[29,30] Our recent structural insights have identified the formation of a unique and highly stable p62 UBA dimer ($K_d \sim 6\,\mu$M) which uses a similar binding surface for both dimerization and Ub recognition.[31] As a consequence, these are highly competitive processes, although in this case the dimer appears to be the biologically inactive form of the UBA. This multistep binding process, involving UBA dimer dissociation and UBA−Ub association, suggests that PDB mutations within the UBA domain may affect Ub-binding function either through direct or indirect effects on these equilibria.[4,31] Alternatively, mutations can affect the stability of the p62 UBA domain and its structural integrity such that at cellular temperatures a significant portion of the protein exists in an unfolded state.[32] Indeed, an additive combination of these factors is likely to be significant.

We describe structural (NMR) and biophysical studies of the C-terminal UBA domain of p62 carrying the common PDB mutations P392L, S399P, M404V/T, G411S, and G425R which have been shown to interfere with the Ub-binding properties of the full-length p62 protein.[1,3,33,34] We show that, in the context of the isolated UBA domain, dysregulation of Ub-binding by PDB mutations may occur via a combination of different mechanisms. However, the most frequently occurring mutation (P392L), found in the majority of PDB patients with *SQSTM1* mutations,[33] has little impact on binding affinity, suggesting more complex mechanisms of ubiquitin recognition within the full-length protein.

MATERIALS AND METHODS

Protein Expression and Purification. The expression and purification of the p62 UBA domain (residues 387−436) and Ub, both unlabeled and fully $^{13}C/^{15}N$-labeled, have been

Received: January 18, 2011
Revised: April 25, 2011
Published: April 25, 2011

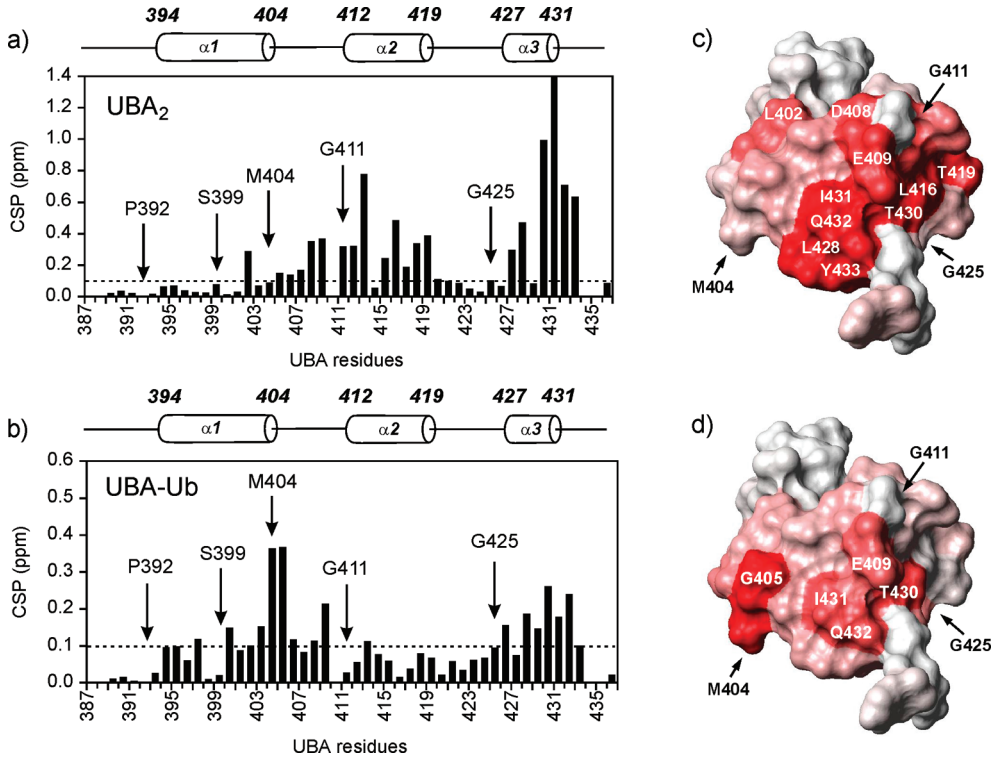

Figure 1. Chemical shift perturbation (CSP, weighted average from ^{1}H and ^{15}N shifts) data for *wt*-UBA showing (a) residues that are perturbed at the dimer interface in the monomer−dimer equilibrium and (b) as a result of the *wt*-UBA binding interaction with ubiquitin (b). The CSPs for the residues at the PDB mutation sites are highlighted with arrows, and the protein secondary structure alignment is shown along the top of each figure. UBA surface showing CSPs to residues involved in dimer formation (c) and in binding Ub (d); darker red represents bigger CSP values (PDB structure 2jy7).

described previously, as has the G425R domain mutant.[4,31] The UBA PDB mutants were prepared by site-directed mutagenesis of the wild-type GST-UBA constructs using previously described protocols.[4,31,32] The longer p62 (341−440) constructs and mutants were expressed and purified using the same protocols. All of the proteins were stored as lyophilized material.

CD and ITC Experiments. Far UV-CD spectra were collected on an Applied PhotoPhysics Pi-star-180 spectrophotometer with a Peltier heating device for melting studies. In equilibrium studies the temperature was regulated using a Neslab RTE-300 circulating programmable water bath, and spectra were collected using either a 1 mm (20−150 μM solutions) or 10 mm (1−10 μM solutions) path length quartz cuvette over a wavelength range from 215−340 nm. The T_m values are the apparent midpoints calculated from the first derivative of the CD melting profiles.

Isothermal titration calorimetry was performed on a MicroCal VP-ITC instrument. UBA stock solution of 270 μM in 50 mM potassium phosphate buffer and 50 mM NaCl (pH 7.0) was injected sequentially (5 μL) into the ITC cell at 298 K (volume 1.424 mL), and the endothermic heat pulse was measured. Data were corrected for the effects of buffer mixing by including an enthalpy of mixing as an iterated variable. The data were analyzed using the MicroCal Origin software to determine K_{dim} and ΔH_{dim} using a standard nonlinear least-squares regression analysis.[31]

NMR Assignments and Titration Experiments. Detailed backbone assignments for a number of p62 UBA mutants were obtained from a variety of 2D and 3D heteronuclear correlation experiments using doubly ^{13}C/^{15}N-labeled UBA samples (300−600 μM), as previously reported for wt-UBA.[4,30] Protein

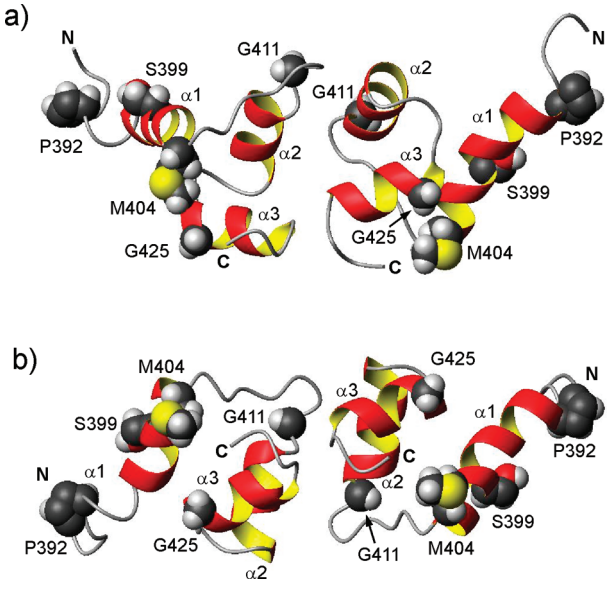

Figure 2. UBA dimer structure (PDB accession code: 2knv) with the PDB mutation sites P392L, S399P, M404, G411S, and G425R highlighted in two different orientations (a, b) related by 90° rotation.

solutions contained 50 mM potassium phosphate buffer and 50 mM NaCl (0.02% sodium azide and 10% D_2O, pH 7.0), and NMR data were collected on an AVANCE600 Bruker spectrometer using standard pulse sequences with Watergate solvent suppression. NMR titration studies with unlabeled Ub were conducted at 298 K by collecting HSQC spectra on ^{15}N-UBA

dx.doi.org/10.1021/bi200079n |*Biochemistry* 2011, 50, 4665–4674

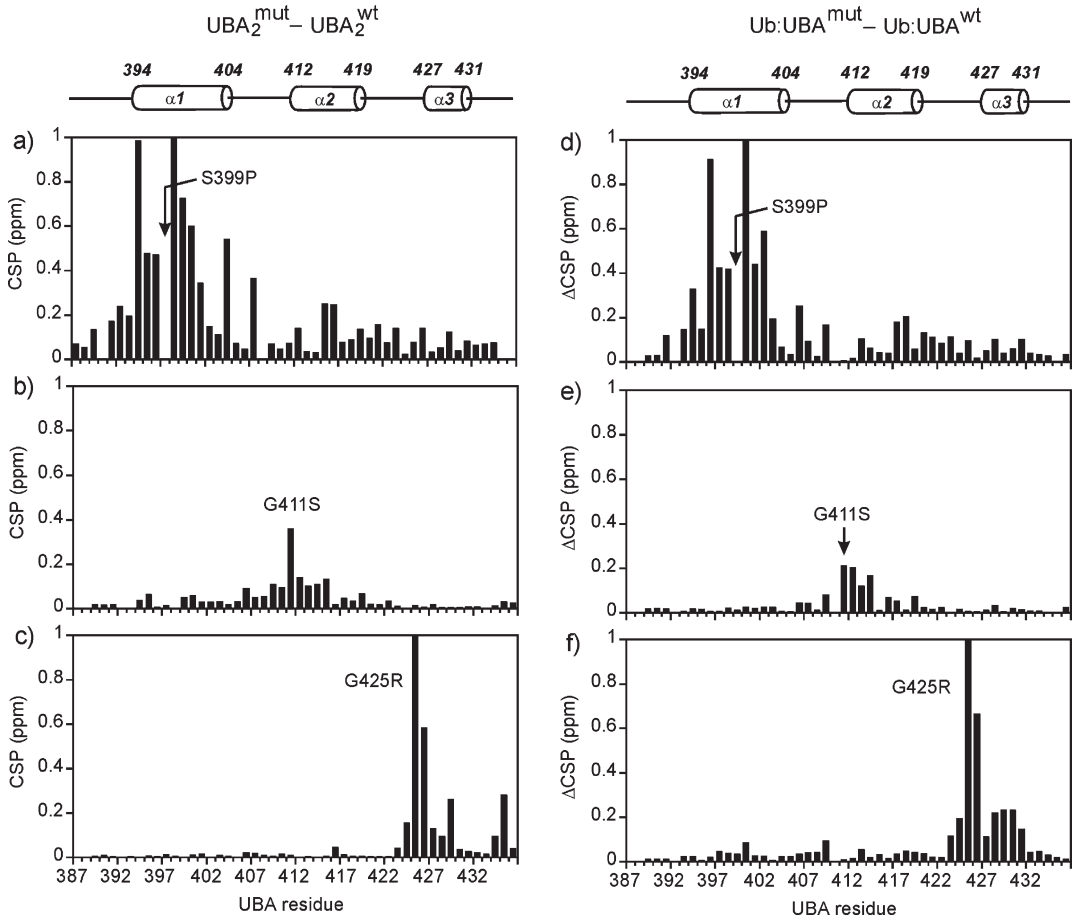

Figure 3. Chemical shift perturbations (CSPs) showing effects of PDB mutations on the structure of the UBA dimer (a–c) and on Ub binding to the UBA monomer (d–f), expressed as the difference between CSPs in the *wt*-UBA dimer and mutant UBA dimer and between *wt*-Ub-UBA complex and mutant UBA–Ub complex, respectively.

up to a 6:1 ratio of Ub:UBA. Titrations with ^{15}N-Ub were also conducted by adding similar excess ratios of unlabeled UBA. Chemical shift perturbations (CSPs) were calculated as $\Delta\delta_{HSQC} = [(\Delta\delta_H)^2 + (\Delta\delta_N/5)^2]^{1/2}$, where $\Delta\delta_H$ and $\Delta\delta_N$ are the observed shifts in the ^{1}H and ^{15}N dimension of the HSQC spectrum, and binding isotherms were constructed and analyzed from the dependence of $\Delta\delta_{HSQC}$ on $[Ub]_{TOT}$. CSPs (>0.05 ppm) were globally fitted to a 1:1 binding model (a total of 31 curves) using the program IGOR Pro (V5.0.5.7 WaveMetrics) to derive an apparent K_{obs}. DynaFit (V3.28.070, Biokin)[35] was used to model K_{obs} in terms of both the K_{dim} and K_d using the experimentally determined K_{dim} values derived from ITC measurements (where $K_{obs} = K_d^2/K_{dim}$).

RESULTS

Mapping PDB Mutation Sites onto the p62 UBA Dimerization and Ub-Binding Surfaces. NMR studies with ^{15}N-labeled p62 UBA have enabled CSP methods to be used to map UBA surface binding residues involved in the formation of both the UBA dimer and the complex of the monomeric UBA with Ub (Figure 1a,b). The two surfaces overlap (Figure 1c,d), making common use of some residues in loop 1 and at the end of helix 3, indicating that dimerization and Ub-binding are competitive processes.[31] The positions of the PDB mutation sites P392, S399, M404, G411, and G425 are shown on the dimer structure in Figure 2a,b. The CSP values associated with each of these residues (Figure 1a,b) provides some measure of their potential involvement in binding interactions. In the context of dimer formation (Figure 1a), CSPs < 0.1 ppm are typical for these residues, with the exception of G411 at the C-terminus of loop 1 (CSP ~ 0.3 ppm).

NMR Examination of the Effect of PDB Mutations on the p62 UBA Dimer Interface. Backbone ^{1}H and ^{15}N assignments for >95% of nonprolyl amide groups of the PDB mutants P392L, S399P, G411S, and G425R were obtained using similar 3D NMR protocols to those described for *wt*-UBA.[4,31] The data provide a basis for a detailed examination of the impact of the mutations on the dimer structure. Although the M404V/T mutants were included in the initial analysis, these variants were associated with poor expression levels, lower solubility, and aggregation effects consistent with a large destabilization of the UBA structure and could not be characterized to the same level of structural detail. The CSP effects of the PDB mutations are shown in Figure 3a–c, with the effects mapped to the dimer structure in Figure 4a–c to demonstrate the propagation of the perturbations from the mutation site.

The P392L mutation occurs at the N-terminus of helix 1 and is remote from both the dimer interface and the Ub-binding surface of the UBA domain and produces minor highly localized structural perturbations (data not shown). In contrast, the S399P substitution at the center of helix 1 has a major impact

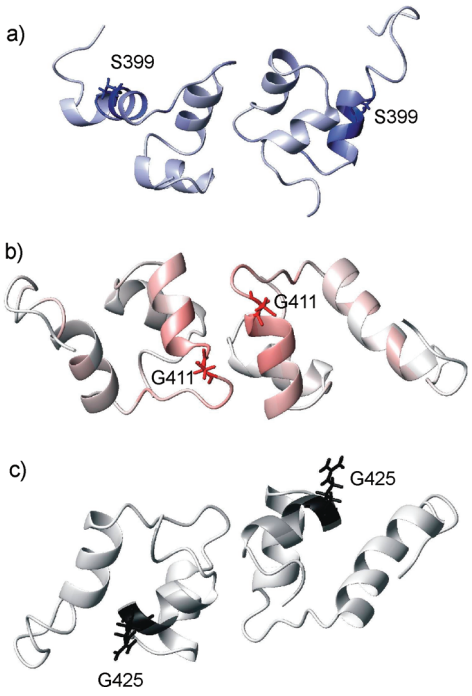

Figure 4. Dimer structures with key PDB mutation sites highlighted. CSP effects from each of the PDB mutations are shaded according to the magnitude of the effect (a) S399P, (b) G411S, and (c) G425R. The CSP data for P392L are not shown because the CSP effects are small; the low stability and solubility of the M404V mutant did not permit a detailed analysis.

on protein secondary structure. A contiguous set of large CSPs (many >0.4 ppm) are seen extending from L394 and S403, encompassing the entirety of helix 1 (Figures 3a and 4a). Moreover, changes in conformation within helix 1 are reflected in significant CSPs for L417 and Q418 in helix 2 which packs against the N-terminus of helix 1. The loss of sequential NH_i-NH_{i+1} NOE connectivities between residue S397-M401 and significant Hα chemical shift deviations from those of wt-UBA toward random coil values, are consistent with helical instability caused by the S399P mutation which extends into loop 1 where perturbations are observed to M404 and F406 (within the MGFS Ub-binding motif) and within the aromatic side chain of W412. Perturbations to tertiary interactions between helices suggest some partial loss of structural integrity within the UBA domain which affects the dimer interface.

The G411S PDB mutant shows evidence for some modest CSPs (~0.1 ppm) in loop 1 preceding the mutation site and within helix 2 immediately following the mutation site, indicating that small perturbations are propagated along loop 1 (Figures 3b and 4b). Small CSPs for several aromatic residues (particularly W412) are evident which suggest perturbations to core packing interactions in the loop conformation preceding helix 2. Although there is no evidence for gross structural changes, the double-Gly insertion within loop 1 of the p62 UBA domain (G410/G411) is a unique structural feature not observed in other UBA domains and plays a key role in stabilizing the p62-UBA dimer interface (Figure 2a,b).[31] In the case of the G425R mutation, which lies at the C-terminus of loop 2 and close to the N-terminus of helix 3, the largest CSPs are highly localized to the mutation site and immediately adjacent sites (Figures 3c and 4c). However, CSPs of ~0.2 ppm are evident within the first turn of helix 3, which may reflect steric contacts associated with accommodating the bulky Gly → Arg side-chain substitution in this position.

CD Studies of Effects of PDB Mutations on p62 UBA Dimerization and Stability. Equilibrium far-UV CD spectra showed the same classical helical spectrum for the P392L, S399P, M404V/T, G411S, and G425R mutants observed for *wt*-UBA. Thermal stabilities were determined by monitoring the change in ellipticity at 222 nm in the range 283−368 K (Figure 5a). The apparent T_m for the transition was calculated at a range of concentrations between 1 and 200 μM. All PDB mutants of the p62-UBA give strong negative bands at 222 and 208 nm, and as observed for the *wt*-UBA of p62, the ratio of $\theta_{222}/\theta_{208}$ shows a clear concentration dependence which is relatively invariant at high concentration then reduces from ~1.1 to around 0.9 at low μM concentrations, consistent with a structural transition (dimer to monomer) in the low micromolar range (5−20 μM). The only exception to this is the G425R mutant which shows only a weak concentration dependence in the $\theta_{222}/\theta_{208}$ ratio (>1) evident within the accessible concentration range, consistent with a highly stable dimer. Equilibrium unfolding experiments were also performed on the P392L mutant in which the substitution occurs close to the N-terminus of the p62-UBA construct (387−436). In this case, a longer p62 (341−440) construct was used. As a control, the T_m values of the *wt*-UBA (386−436) and p62 (341−440) constructs were studied and found to have indistinguishable stabilities. The insertion of the P392L mutation had a small impact on the stability of the UBA domain.

The observed T_m values for the *wt*-UBA and mutant p62-UBA domains vary with concentration in an approximately sigmoidal manner, with the high concentration plateau representing the T_m of the dimer and the low concentration values that of the monomeric UBA.[30] The changes in stability with respect to *wt*-UBA, and the relative stabilities of the monomer and dimer, are captured in the limiting T_m values and in the separation of the upper and lower limits (Figure 5b). The P392L mutant shows little variation from *wt*-UBA; however, the S399P, M404V/T, and G411S mutants show a significant reduction in T_m values of >20 K at high concentrations and by >18 K at low concentrations, indicating that both the monomer and dimer states are destabilized as a result of these mutations. In contrast, the G425R mutant shows an increase in stability of both the dimer and monomer of 5−7 K. The limited change in the ratio of $\theta_{222}/\theta_{208}$ suggests that the full shift to the monomeric form is not accessible in this concentration range.

In Table 1, we have estimated from the CD melting studies the fraction folded (ϕ_f) at 310 K (physiological temperature) for each of the mutants at low protein concentrations where the monomer is in equilibrium with the unfolded state. In the case of S399P, M404V/T, and G411S, the loss of stability results in a significant fraction present in the unfolded form. The *wt*-UBA, P392L, and G425R mutants appear to be fully folded and in the case of G425R still partially dimeric under these conditions.

ITC Studies of Effects of PDB Mutations on p62 UBA Dimer Stability. Quantitative dimer stability data were obtained from ITC dilution experiments recorded on 270 μM protein samples of the UBA domains by sequential injection into buffer solution.[30] The resulting dissociation isotherm from the integrated heat response was fitted to a dimer dissociation model to determine K_{dim} and ΔH_{dim} (Figure 5c,d). The dissociation isotherms for wt-UBA in the (386−436) and (341−440)

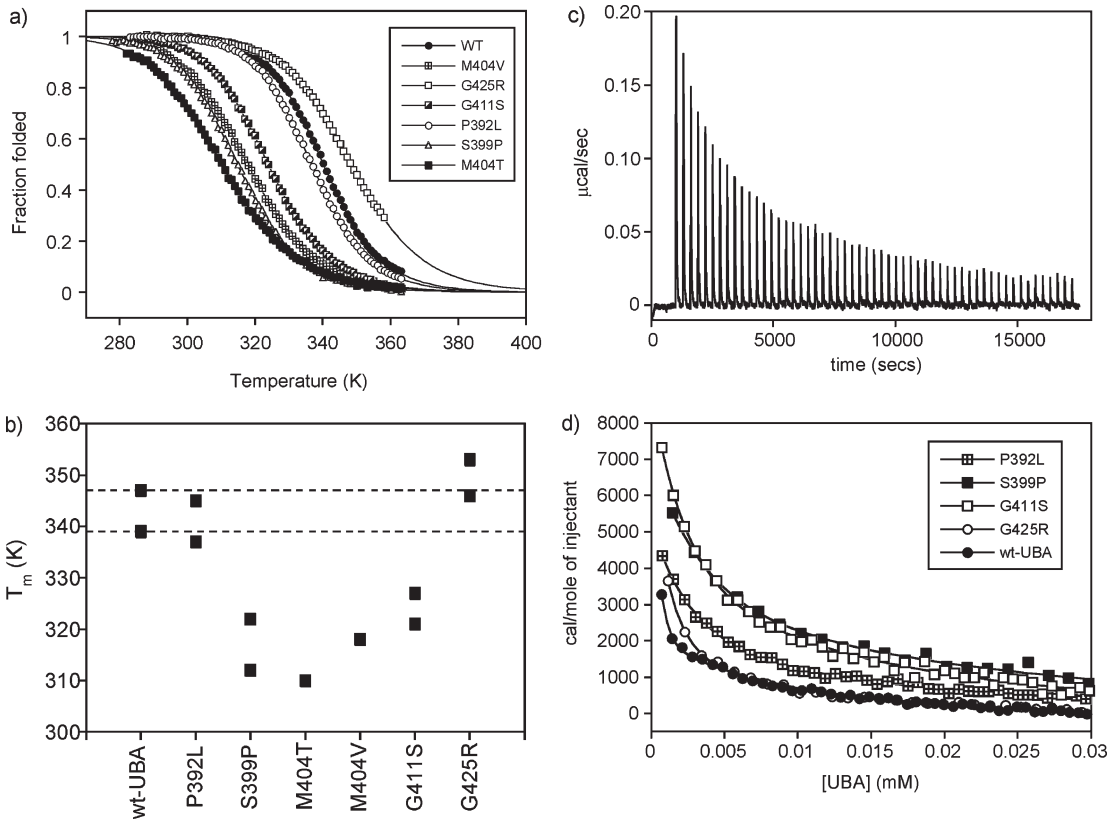

Figure 5. (a) CD thermal unfolding curves, shown as the fraction of folded protein, for *wt*-UBA and PDB mutant UBA domains at 5 μM concentration where the proteins are essentially monomeric (the exception being the G425R mutant). Lines of best fit to a two-state folding model are shown. (b) Concentration dependence of the T_m values from CD studies showing upper and lower limits of thermal stability over the concentration range for each mutant of 1−200 μM. The low concentration limit (lower T_m) represents the stability of the monomer, and at high protein concentrations (high T_m) the stability of the dimer (errors of ±1 K are shown by the size of the data point). The dotted lines represent the limiting values for *wt*-UBA as a reference point. In the case of M404T and M404V, only the low concentration T_m values could be determined with any certainty. (c) Representative ITC dilution profile for G411S showing the endothermic heat pulses from the sequential dilution of 5 μM aliquots of a 270 μM stock solution in to buffer solution at 298 K. (d) Dilution isotherms are shown for all of the PDB mutants and were fitted to a dimer−monomer equilibrium to determine K_{dim} values (see Table 1).

Table 1. Changes in Thermal Stability and Fraction Folded Determined by CD Melting Studies and Thermodynamic Parameters for Dimer Dissociation of the p62-UBA Domain and PDB Mutants Determined by ITC at 298 K

UBA construct	ΔT_m (K)[a]	ϕ_f(310 K)[b]	K_{dim} (μM)[c]	ΔH_{dim} (kJ/mol)	ΔG_{dim} (kJ/mol)
UBA (386−436)		0.98	7.1 ± 1.0	6.8 ± 3	29.4 ± 1
UBA (341−440)	+0.5	0.98	7.6 ± 1.0	13.4 ± 4	29.4 ± 1
P392L (341−440)	−4.1	0.98	9.6 ± 0.8	10.3 ± 2	28.6 ± 1
S399P	−26.0	0.64	17.5 ± 3.0	13 ± 1.5	27.2 ± 1
M404V	−23.1	0.75	nd	nd	nd
M404T	−30.6	0.51	nd	nd	nd
G411S	−16.9	0.88	10.6 ± 0.7	16.7 ± 2	27.4 ± 1
G425R	+7.7	0.99	3.0 ± 0.9	16 ± 4	31.5 ± 1

[a] CD melting studies ($\Delta T_m = T_m^{mut} - T_m^{wt}$). [b] Fraction folded at 310 K calculated from CD melting curves. [c] Equilibrium dimer dissociation constant (K_{dim}), enthalpy (ΔH_{dim}), and free energy of dissociation (ΔG_{dim}) determined from ITC dilution studies at 298 K; nd = not determined; errors were determined from the nonlinear least-squares analysis.

constructs where essentially identical (see Table 1), indicating that the additional unstructured 45 residues at the N-terminus of the p62 UBA (341−440) is not influencing the stability of the dimer. The calculated K_{dim} values for the PDB mutant UBA domains are consistent with the observed protein concentration-dependent changes in $\theta_{222}/\theta_{208}$ ratios observed by far-UV CD.

The G411S mutation produced a marginal reduction in dimer stability (K_{dim} = 10 ± 0.7 μM), with a more significant effect apparent for S399P (K_{dim}= 17 ± 3 μM). The P392L mutation showed a marginally reduced stability with K_{dim} = 9.8 ± 0.7 μM; however, G425R results in further stabilization of the dimer (K_{dim} = 3 ± 0.9 μM).

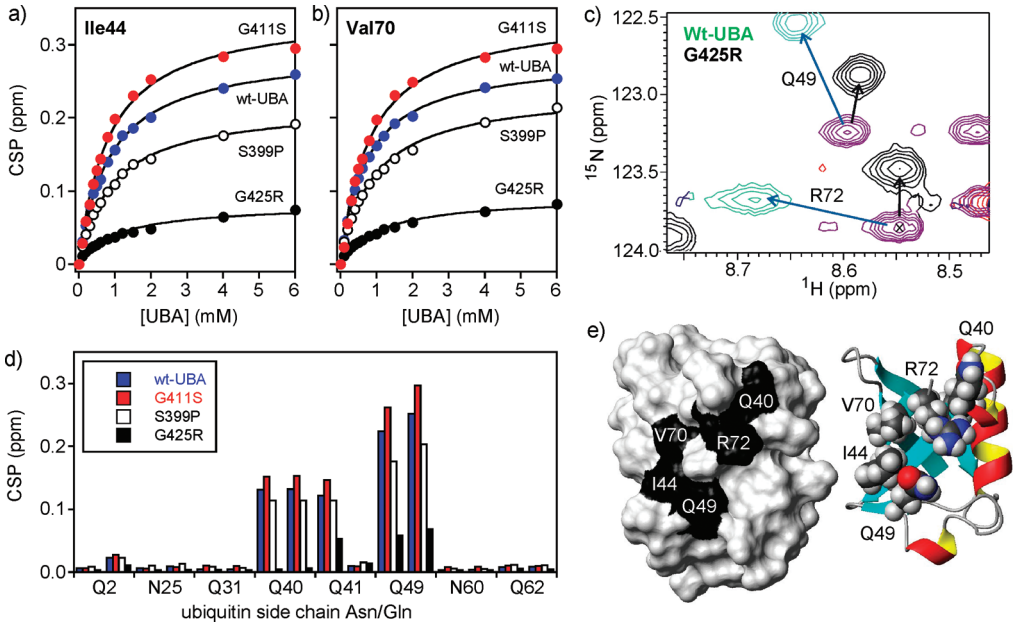

Figure 6. Binding isotherms for *wt*-UBA and PDB mutant UBA domains derived from fast-exchange NMR CSP effects on the resonances of (a) I44 and (b) V70 of ^{15}N-Ub. Differences in the magnitude of the binding shifts (limiting CSP values) are evident for the different mutants, with G425R showing the weakest interaction. (c) Portion of the ^{1}H/^{15}N-HSQC spectra of ^{15}N-Ub in the presence of *wt*-UBA and the G425R mutant showing differences in the perturbations to Q49 and R72. (d) Limiting CSPs for the pairs of resonances of the side-chain NH_2 groups of Asn and Gln residues of ^{15}N-Ub. Significant perturbations to Q40, Q41, and Q49 are observed with *wt*-UBA indicative of side-chain involvement in UBA binding. Similar binding effects are evident for interactions with the S339P and G411S mutants; however, these are significantly diminished for G425R with complete loss of interaction with Q40. (e) Highlighted residues mapped to the surface of Ub using a CPK and ribbon representation in the same orientation. The unstructured C-terminal residues 73−75 have been removed for clarity.

Table 2. Apparent Dissociation Constants for Ubiquitin Binding (K_{obs}) and Actual K_d Values for the p62-UBA and PDB Mutants[a]

UBA construct	K_{obs} (μM)[b]	K_d (μM)[c]	ΔG^{mono}_{298} (kJ/mol)	$\Delta\Delta G^{mono}_{298}$ (kJ/mol)
UBA (387−436)	741 ± 80	42 ± 3	−25.0 ± 0.2	
UBA (341−440)	500 ± 60	20 ± 4	−26.7 ± 0.3	−1.7 ± 0.3
P392L (341−440)	658 ± 60	35 ± 3	−25.4 ± 0.2	−0.4 ± 0.2
S399P	991 ± 90	140 ± 16	−22.0 ± 0.2	3.0 ± 0.3
M404V/T	nd	nd	nd	nd
G411S	800 ± 80	43 ± 4	−25.0 ± 0.1	0 ± 0.2
G425R	1430 ± 200	340 ± 100	−19.8 ± 0.9	5.2 ± 0.9

[a] ΔG for binding was determined from the measured affinity constants; the $\Delta\Delta G$ for PDB mutants were also determined. [b] Apparent dissociation constant K_{obs} determined from NMR titration data and represents the competitive effects of dimer association and ubiquitin binding. [c] K_d for binding monomeric UBA to Ub.

Effects of the PDB Mutations on the Ub-Bound Structure of the p62 UBA Domain. NMR CSP methods were previously used to map the Ub-binding surface of the monomeric ^{15}N-labeled UBA (Figure 1b), implicating loop 1 and the C-terminus of helix 3 in forming the Ub-binding patch on the UBA.[31] Of all the PDB mutations considered, only M404 appears to be in direct contact at the Ub-binding interface (CSP > 0.1 ppm, see Figure 1) and is associated with a substantial Ub-induced CSP of >0.3 ppm. In particular, P392 at the N-terminus of helix 1 and S399 at the center of helix 1 are more remote from the Ub-binding surface of the UBA domain. G411 is immediately adjacent to the highly conserved loop 1 MGFS binding motif (residues 404−407) found in many UBA domains.[36,37] G425 is located in loop 2 close to the N-terminus of helix 3 and distal to the Ub-binding residues located at the C-terminus of helix 3.

Titrations of the ^{15}N-labeled UBAs (1 mM) with Ub (up to 6−8 mM) enabled us to examine the effects of PDB mutations on the bound structure of the monomeric UBA. In all cases, a slow exchange binding event was seen with the pattern and magnitude of CSPs indicative of the two-step process of dimer dissociation and Ub-binding evident for *wt*-UBA. In the case of the G425R mutant, the binding interaction is weak and the titration does not reach saturation in the accessible concentration range of Ub (8 mM), resulting in residual peaks for the uncomplexed UBA dimer.

The mutation-induced differences in CSPs (ΔCSPs) between the Ub-bound *wt*-UBA versus Ub-bound PDB mutants largely mirror the perturbations evident for the dimer structures (Figure 3d−f). Mutation-induced bound ΔCSPs for the G411S mutant appear to only affect residues for which intrinsically small

binding-induced CSPs are evident. In contrast, the S399P mutation causes significant bound ΔCSP effects across the entire domain, suggesting that the large changes in conformation in helix 1 of the UBA evident in the dimer structure are also evident in the Ub-bound form and are not "rescued" by the binding interaction (Figure 3d). The structural impact of the S399P mutation produces CSP effects which are larger than those that arise from the binding interaction alone (contrast Figures 1b and 3d).

In the case of the G425R mutant, the observed ΔCSPs (many 0.1−0.2 ppm) appear to extend along most of helix 3 to include those residues at the C-terminus identified as part of the Ub-recognition surface (T430 and I431; Figure 3f). The G425R substitution at the N-terminus of helix 3 appears to sterically interfere with the complementarity of the UBA-Ub binding surface with effects propagated along helix 3. However, the G425R substitution does not affect contacts involving the MGFS motif in loop 1 (residues 404−407) where CSPs are similar to those for *wt*-UBA (ΔCSPs < 0.05 ppm).

PDB Mutations Perturb Ub Binding Interactions. The effects of the PDB mutations on the UBA binding interface were studied in NMR titrations with ^{15}N-labeled Ub to map changes to the interaction surface of Ub. p62-UBA (up to 6 mM) was titrated into 1 mM ^{15}N-Ub, and a series of ^{1}H/^{15}N-HSQC spectra demonstrated concentration-dependent fast-exchange CSPs for many of the Ub resonances. This exchange regime readily facilitates the assignment of the fully bound state of ^{15}N-Ub, although a few resonances (Arg42, Lys48, and Leu71) shift and broaden upon titration with *wt*-UBA with complete signal loss at a UBA:Ub ratio of 0.2:1. The CSP data for *wt*-UBA were used to derive binding isotherms for the UBA-Ub interaction. CSPs (>0.05 ppm) were globally fitted to a 1:1 binding model (a total of 31 curves), yielding K_{obs} = 741 ± 80 μM. Subsequently, we used a competitive equilibrium model to determine the dissociation constant for Ub-binding to the monomeric UBA (K_d) using the experimentally determined ITC values for the dimer dissociation constant (K_{dim}), giving a K_d = 42 ± 3 μM for the p62-UBA:Ub interaction.

NMR titrations were extended to the PDB mutants S399P, G411S, and G425R. The magnitude of the CSPs observed at saturation (6 mM UBA) are shown in Figure 6a,b for I44 and V70, which form part of the Ub hydrophobic surface binding patch.[4,31] In the case of the G425R mutant, the CSPs are particularly small, consistent with a much weaker interaction. The line broadening effects previously noted in titration studies for residues Arg42, Lys48, and Leu71 are less significant for the PDB mutants, although their large CSPs are consistent with close proximity to the UBA binding surface.

Although the CSPs for ^{15}N-Ub with the various PDB mutants suggest binding to the same surface, the S399P and G425R mutants highlight some noticeable differences. In the case of the S399P mutant, the surface cluster of residues Leu43, Ala46, Gly47, and Gln49 show additional perturbations arising indirectly from changes in interactions in the region of loop 1 of the UBA domain which are propagated from the S399 mutation site in helix 1. In the case of the G425R mutant, differences are clearly evident for Arg72, Gln49 (Figure 6c) and the side-chain NH_2 of Gln40 of Ub. The side chains of Gln40, Gln41, and Gln49 are all perturbed upon binding *wt*-UBA and to comparable extents by the mutants S399P and G411S (Figure 6d). However, Gln40 shows a loss of interaction with the G425R mutant, with much diminished effects for Gln41 and Gln49. The colocalization of these residues on the Ub surface is shown in Figure 6e, all of which appear to be in close proximity to E409 on the UBA binding face. It is not apparent from modeling studies that the G425R mutation leads directly to unfavorable contacts at the Ub binding surface. However, R425 has the opportunity to engage with the flexible E409 side chain to form a non-native salt bridge within the UBA dimer. This electrostatic interaction could explain the increase in stability of the G425R UBA dimer (Table 1) and the observed perturbations to the intermolecular interactions of E409 with the Ub binding interface. However, a high-resolution structure of the complex will be required to resolve the exact nature of the perturbations.

NMR-derived binding isotherms from the titration data for the UBA mutants (Figure 6a,b), together with global fitting of the ^{15}N-Ub CSPs, yielded K_{obs} values for the PDB mutants. The ITC-derived values for the dimer stabilities (K_{dim}; see Table 1) were again used to determine Ub-binding affinities (K_d) for the monomeric PDB UBA mutants (Table 2). The most significant reductions in K_d values (3−8-fold) are seen for the S399P and G425R mutants. The G411S mutation shows little effect on Ub-recognition or dimer stability at 298 K, despite significant changes in thermal stability of both the monomeric and dimeric UBA structure (Table 1).

DISCUSSION

Loss of Structural Integrity and Protection against Proteasomal Degradation. In previous studies,[32] we have shown that p62-UBA (like other UBA domains) stabilizes the unstable reporter protein Ub-R-GFP and reduces its susceptibility to proteasomal degradation. Certain missense PDB mutations (associated with loss of Ub-binding *in vitro*) do not stabilize the Ub-R-GFP reporter to the same extent as *wt*-UBA, consistent with reporter stabilization being directly linked to Ub-binding ability.[11] However, in these assays we found that the M404T mutation further destabilized the Ub-R-GFP reporter. Moreover, when M404T was inserted in the stable Ub-M-GFP reporter protein (which lacks a degradation signal), it also promoted degradation of Ub-M-GFP. This suggests that the M404T mutant is not only unable to protect a proteasomal substrate from degradation but functions itself as a degradation signal.[38] Accordingly, when Ub-R-UBA-M404T was expressed in a yeast strain that lacked the Ubr1 Ub-ligase responsible for recognition and ubiquitylation of N-end rule substrates, the protein remained unstable, suggesting that it is targeted by an additional pathway for degradation. Together these observations would suggest that the UBA-M404T mutant is severely misfolded and recognized by the protein quality control systems, at least in yeast. This is supported by CD studies which show that the M404T mutant UBA domain has considerable thermal instability with an estimate of the fraction of folded protein at 310 K of only ∼50%.

In the context of PDB, we infer that although this change occurs at the Ub-binding interface it probably exerts its effects on p62 function via destabilization/misfolding of the UBA domain at physiological temperatures, an effect which appears to be unique to the M404T mutation. Indeed, our data show that mutant UBA domains with the greatest protective effects in the reporter assays were those that were the most thermally stable, indicating that structural integrity may play some part in regulating degradation by the proteasome.[32] However PDB-associated

Table 3. Impact of Paget's Disease Mutations on UBA Structural Integrity, Dimer Stability, and Ubiquitin Binding Interface[a]

	P392L	S399P	M404V(T)	G411S	G425R
location of mutation	N-cap of helix 1	helix 1	loop 1	loop 1	loop 2
structural integrity	–	↓↓	↓↓↓ (nd)	↓	↑
change in thermal stability	–	↓↓	↓↓ (↓↓↓)	↓↓	↑
impact on dimer stability (ITC)	–	↓	nd	–	↑
effect on Ub-binding interface	–	–	↓↓↓ (↓↓↓)	–	↓↓
effects on Ub-binding affinity in NMR titration studies	–	↓↓	nd	–	↓↓↓
binding in pull-down assays	–	↓	↓↓↓ (↓↓↓)	–	↓↓↓
effects of PDB mutations in full-length p62 on Ub-binding	↓	↓	↓↓↓ (↓↓↓)	↓	↓↓↓

[a] (–) indicates small or no effect from mutation; the number of arrows indicates an increase (↑) or decrease (↓) in relation to data reported in Tables 1 and 2 and from pull-down assays of isolated UBA domains reported elsewhere (see refs 3, 6 ,and 45) (nd = not determined), but effects of M404V/T on structural integrity, dimer stability, and Ub-binding affinity are significant.

mutations were not observed to have any effect on p62 turnover in human cells, suggesting that the mutations within the UBA domain in general do not play a significant role in rendering the p62 protein more susceptible to proteasomal degradation *in vivo*.

Biological Context of the Impact of PDB Mutations in the p62 UBA Domain. A number of studies have implicated UBDs in the formation of biologically important homo- and heterodimeric structures which enhance or regulate Ub-binding,[29,30,39,40] although in general relatively little attention has been paid to the functional importance of dimerization. In this sense, the p62 UBA domain is unique in that the UBA dimer is not the functional form but appears to regulate Ub-binding because dimerization and Ub recognition are competitive processes.[31] Since the Ub-binding function of p62 is indispensable for its ability to regulate NF-κB signaling[10] and autophagy,[41] there is the strong implication that dimerization must be physiologically relevant for these processes. We have recently demonstrated that engineered point mutations in p62 which destabilize the UBA dimer interface (E409K and G410K) lead to a higher proportion of the bound monomer in *in vitro* experiments and in reporter assays are associated with reduced NF-κB activity compared with *wt*-p62.[31] Moreover, we have shown that the naturally occurring G425R UBA mutation, which is linked to PDB with the corresponding mutation, also exerts its effects on Ub-binding and the regulation of NF-κB signaling by affecting UBA dimerization. The present study both verifies this previous observation and extends it by providing a quantitative analysis of these two processes which, in concert, lead to a significant reduction in Ub-binding affinity.

The PDB mutants P392L, S399P, G411S, and G425R, and to a lesser extent M404V/T, have all been investigated in the context of *in vitro* studies of isolated p62 UBA domain constructs to determine their effects on Ub recognition. S399P and G425R have a quantifiable impact on Ub-binding affinity which we have rationalized from a detailed structural perspective. It is evident that mutations at the M404 site (V or T) lead to the greatest loss of stability (see Figure 4) and reduction in Ub-binding affinity,[4,6] which proved difficult to quantify. The M404 → V or T mutations occur within the conserved loop 1 MGFS binding motif and directly impact on both Ub-binding affinity and the structural integrity of the UBA. The S399P mutation appears to demonstrate how long-range structural instability arising from disruption of helix 1 can modulate Ub-binding affinity through loss of structural integrity; however, the loss of both dimer stability and Ub-binding affinity is surprisingly relatively modest (~3-fold) in the context of the isolated UBA domain.

In contrast, the G425R mutant appears to enhance dimer stability affecting the population of the monomer at equilibrium while simultaneously perturbing the UBA—Ub interface. The clinically most frequently observed PDB mutation (P392L) lies at the N-terminus of helix 1[5] and is remote from the dimer interface and the Ub-binding site and is found to have minimal impact on UBA dimer stability or on Ub recognition. In contrast, all of the examined PDB UBA mutants attenuate polyUb binding in pull-down assays in the context of the full-length p62 (1—440), suggesting that although the C-terminal UBA domain is a prerequisite for Ub-binding other factors play some as yet unspecified role in regulating the interaction of p62 with polyUb chains.[3] The observation that PDB mutations have now been identified that lie outside of the UBA domain supports this hypothesis.[2]

CONCLUSIONS

No single mechanism appears to unambiguously account for loss of Ub-binding affinity associated with PDB mutations. Indeed, we see evidence for loss of structural integrity, both stabilization and destabilization of the UBA dimer structure, both direct and indirect effects on the UBA-Ub binding interface, and a combination of all of these factors (summarized in Table 3). Notably, the P392L and G411S mutations have minimal effects on the mechanisms described. At the molecular and functional level, our objective is to understand how weak p62-UBA/Ub interactions are "levered" into physiologically relevant high-affinity interactions and how the relatively modest effects of PDB mutations on the various recognition events may be amplified. The oligomeric nature of p62 appears to be essential for its function[42] and suggests how small perturbations at the individual UBA level can be amplified through avidity effects as the multiple UBA domains of the oligomeric p62 simultaneously interact with a polyUb chain.[31,43]

A further long-term objective is to definitively establish whether alterations in Ub-binding function of PDB mutant p62 proteins are directly related to the disease severity in patients with the corresponding mutations.[33] Such a relationship would provide further supportive evidence of a central role of p62/*SQSTM1* gene mutations in PDB pathogenesis[34,44] and may help explain the wide phenotypic variation of disease severity in PDB patients with *SQSTM1* mutations. In a previous study,[45] we saw only a very small difference in extent of disease when mutations were grouped according to their effect on Ub-binding in the

context of the isolated UBA domains in pull-down assays. Such function-phenotype correlations are likely to be most informative using functional data derived for full-length p62 proteins.

AUTHOR INFORMATION

Corresponding Author

*E-mail: mark.searle@nottingham.ac.uk. Tel: (44) 115 951 3567. Fax: (44) 115 846 6059.

Funding Sources

We thank the BBSRC (UK) for funding to M.S.S. and R.L. and the School of Chemistry and the EPSRC (UK) for supporting T.P.G.

ACKNOWLEDGMENT

We are grateful to Drs. Barbara Ciani and Thomas Gallagher for contributions at an early stage of this project to stability studies of PDB mutants of the p62 UBA domain.

ABBREVIATIONS

PDB, Paget's disease of bone; SQSTM1, sequestosome 1; UBA, ubiquitin associated domain; Ub, ubiquitin; polyUb, polyubiquitin; CD, circular dichroism; NMR, nuclear magnetic resonance; HSQC, heteronuclear single quantum coherence; ITC, isothermal titration calorimetry; GFP, green fluorescent protein; CSP, chemical shift perturbation.

REFERENCES

(1) Layfield, R., Ciani, B., Ralston, S. H., Hocking, L. J., Sheppard, P. W., Searle, M. S., and Cavey, J. R. (2004) Structural and functional studies of mutations affecting the UBA domain of SQSTM1 (p62) which cause Paget's disease of bone. *Biochem. Soc. Trans. 32*, 728–730.

(2) Najat, D., Garner, T., Hagen, T., Shaw, B., Sheppard, P. W., Falchetti, A., Marini, F., Brandi, M. L., Long, J. E., Cavey, J. R., Searle, M. S., and Layfield, R. (2009) Characterization of a non-UBA domain missense mutation of sequestosome 1 (SQSTM1) in Paget's disease of bone. *J. Bone Miner. Res. 24*, 632–642.

(3) Cavey, J. R., Ralston, S. H., Sheppard, P. W., Ciani, B., Gallagher, T. R., Long, J. E., Searle, M. S., and Layfield, R. (2006) Loss of ubiquitin binding is a unifying mechanism by which mutations of SQSTM1 cause Paget's disease of bone. *Calcif. Tissue Int. 78*, 271–277.

(4) Long, J., Gallagher, T. R., Cavey, J. R., Sheppard, P. W., Ralston, S. H., Layfield, R., and Searle, M. S. (2008) Ubiquitin recognition by the ubiquitin-associated domain of p62 involves a novel conformational switch. *J. Biol. Chem. 283*, 5427–5440.

(5) Ciani, B., Layfield, R., Cavey, J. R., Sheppard, P. W., and Searle, M. S. (2003) Structure of the ubiquitin-associated domain of p62 (SQSTM1) and implications for mutations that cause Paget's disease of bone. *J. Biol. Chem. 278*, 37409–37412.

(6) Cavey, J. R., Ralston, S. H., Hocking, L. J., Sheppard, P. W., Ciani, B., Searle, M. S., and Layfield, R. (2005) Loss of ubiquitin-binding associated with Paget's disease of bone p62 (SQSTM1) mutations. *J. Bone Miner. Res. 20*, 619–624.

(7) Goode, A., and Layfield, R. (2010) Recent advances in understanding the molecular basis of Paget disease of bone. *J. Clin. Pathol. 63*, 199–203.

(8) Layfield, R., and Hocking, L. J. (2004) SQSTM1 and Paget's disease of bone. *Calcif. Tissue Int. 75*, 347–357.

(9) Sanz, L., Diaz-Meco, M. T., Nakano, H., and Moscat, J. (2000) The atypical PKC-interacting protein p62 channels NF-kappaB activation by the IL-1-TRAF6 pathway. *EMBO J. 19*, 1576–1586.

(10) Wooten, M. W., Geetha, T., Seibenhener, M. L., Babu, J. R., Diaz-Meco, M. T., and Moscat, J. (2005) The p62 scaffold regulates nerve growth factor-induced NF-kappaB activation by influencing TRAF6 polyubiquitination. *J. Biol. Chem. 280*, 35625–35629.

(11) Seibenhener, M. L., Geetha, T., and Wooten, M. W. (2007) Sequestosome 1/p62 - More than just a scaffold. *FEBS Lett. 581*, 175–179.

(12) Sanz, L., Sanchez, P., Lallena, M. J., Diaz-Meco, M. T., and Moscat, J. (1999) The interaction of p62 with RIP links the atypical PKCs to NF-kappaB activation. *EMBO J. 18*, 3044–3053.

(13) Rea, S. L., Walsh, J. P., Ward, L., Yip, K., Ward, B. K., Kent, G. N., Steer, J. H., Xu, J., and Ratajczak, T. (2006) A novel mutation (K378X) in the sequestosome 1 gene associated with increased NF-kappaB signaling and Paget's disease of bone with a severe phenotype. *J. Bone Miner. Res. 21*, 1136–1145.

(14) Rea, S. L., Walsh, J. P., Ward, L., Magno, A. L., Ward, B. K., Shaw, B., Layfield, R., Kent, G. N., Xu, J., and Ratajczak, T. (2009) Sequestosome 1 mutations in Paget's disease of bone in Australia: prevalence, genotype/phenotype correlation, and a novel non-UBA domain mutation (P364S) associated with increased NF-kappaB signaling without loss of ubiquitin binding. *J. Bone Miner. Res. 24*, 1216–1223.

(15) Feng, Y. F., and Longmore, G. D. (2005) The LIM protein Ajuba influences interleukin-1- induced NF-kappa B activation by affecting the assembly and activity of the protein kinase C zeta/p62/TRAF6 signaling complex. *Mol. Cell. Biol. 25*, 4010–4022.

(16) Seibenhener, M. L., Babu, J. R., Geetha, T., Wong, H. C., Krishna, N. R., and Wooten, M. W. (2004) Sequestosome 1/p62 is a polyubiquitin chain binding protein involved in ubiquitin proteasome degradation. *Mol. Cell. Biol. 24*, 8055–8068.

(17) Geetha, T., Seibenhener, M. L., Chen, L., Madura, K., and Wooten, M. W. (2008) p62 serves as a shuttling factor for TrkA interaction with the proteasome. *Biochem. Biophys. Res. Commun. 374*, 33–37.

(18) Babu, J. R., Geetha, T., and Wooten, M. W. (2005) Sequestosome 1/p62 shuttles polyubiquitinated tau for proteasomal degradation. *J. Neurochem. 94*, 192–203.

(19) Moscat, J., and Diaz-Meco, M. T. (2009) p62 at the crossroads of autophagy, apoptosis, and cancer. *Cell 137*, 1001–1004.

(20) Pankiv, S., Clausen, T. H., Lamark, T., Brech, A., Bruun, J. A., Outzen, H., Overvatn, A., Bjorkoy, G., and Johansen, T. (2007) p62/SQSTM1 Binds Directly to Atg8/LC3 to Facilitate Degradation of Ubiquitinated Protein Aggregates by Autophagy. *J. Biol. Chem. 282*, 24131–24145.

(21) Hurley, J. H., Lee, S., and Prag, G. (2006) Ubiquitin-binding domains. *Biochem. J. 399*, 361–372.

(22) Trempe, J. F., Brown, N. R., Lowe, E. D., Gordon, C., Campbell, I. D., Noble, M. E., and Endicott, J. A. (2005) Mechanism of Lys48-linked polyubiquitin chain recognition by the Mud1 UBA domain. *EMBO J. 24*, 3178–3189.

(23) Kozlov, G., Nguyen, L., Lin, T., De Crescenzo, G., Park, M., and Gehring, K. (2007) Structural basis of ubiquitin recognition by the ubiquitin-associated (UBA) domain of the ubiquitin ligase EDD. *J. Biol. Chem. 282*, 35787–35795.

(24) Swanson, K. A., Hicke, L., and Radhakrishnan, I. (2006) Structural basis for monoubiquitin recognition by the Ede1 UBA domain. *J. Mol. Biol. 358*, 713–724.

(25) Raasi, S., Varadan, R., Fushman, D., and Pickart, C. M. (2005) Diverse polyubiquitin interaction properties of ubiquitin-associated domains. *Nat. Struct. Mol. Biol. 12*, 708–714.

(26) Zhang, D., Raasi, S., and Fushman, D. (2008) Affinity makes the difference: nonselective interaction of the UBA domain of Ubiquilin-1 with monomeric ubiquitin and polyubiquitin chains. *J. Mol. Biol. 377*, 162–180.

(27) Kang, Y., Vossler, R. A., Diaz-Martinez, L. A., Winter, N. S., Clarke, D. J., and Walters, K. J. (2006) UBL/UBA ubiquitin receptor proteins bind a common tetraubiquitin chain. *J. Mol. Biol. 356*, 1027–1035.

(28) Walters, K. J., Lech, P. J., Goh, A. M., Wang, Q., and Howley, P. M. (2003) DNA-repair protein hHR23a alters its protein structure upon binding proteasomal subunit S5a. *Proc. Natl. Acad. Sci. U.S.A. 100*, 12694–12699.

(29) Prag, G., Misra, S., Jones, E. A., Ghirlando, R., Davies, B. A., Horazdovsky, B. F., and Hurley, J. H. (2003) Mechanism of ubiquitin recognition by the CUE domain of Vps9p. *Cell 113*, 609–620.

(30) Peschard, P., Kozlov, G., Lin, T., Ahmad Mirza, I., Berghuis, A. M., Lipkowitz, S., Park, M., and Gehring, K. (2007) Structural basis for ubiquitin-mediated dimerisation and activation of the ubiquitin protein ligase Cbl-b. *Mol. Cell 27*, 474–485.

(31) Long, J., Garner, T. P., Pandya, M. J., Craven, C. J., Chen, P., Shaw, B., Williamson, M. P., Layfield, R., and Searle, M. S. (2010) Dimerisation of the UBA Domain of p62 Inhibits Ubiquitin Binding and Regulates NF-κB Signalling. *J. Mol. Biol. 396*, 178–194.

(32) Heinen, C., Garner, T. P., Long, J., Bottcher, C., Ralston, S. H., Cavey, J. R., Searle, M. S., Layfield, R., and Dantuma, N. P. (2010) Mutant p62/SQSTM1 UBA domains linked to Paget's disease of bone differ in their abilities to function as stabilization signals. *FEBS Lett. 584*, 1585–1590.

(33) Visconti, M. R., Langston, A. L., Alonso, N., Goodman, K., Selby, P. L., Fraser, W. D., and Ralston, S. H. (2010) Mutations of SQSTM1 are associated with severity and clinical outcome in Paget's disease of bone. *J. Bone Miner. Res. 25*, 2368–2373.

(34) Michou, L., Collet, C., Laplanche, J. L., Orcel, P., and Cornelis, F. (2006) Genetics of Paget's disease of bone. *Joint Bone Spine 73*, 243–248.

(35) Kuzmic, P. (2009) DynaFit: a software package for enzymology. *Methods Enzymol. 467*, 247–280.

(36) Mueller, T. D., and Feigon, J. (2002) Solution structures of UBA domains reveal a conserved hydrophobic surface for protein-protein interactions. *J. Mol. Biol. 319*, 1243–1255.

(37) Diekmann, T., Withers-Wand, E. S., Jarosinski, M. A., Liu, C.-F., Chen, I. S. Y., and Feigon, J. (1998) *Nat. Struct. Biol. 5*, 104–107.

(38) Heinen, C., Acs, K., Hoogstraten, D., and Dantuma, N. P. (2011) C-terminal UBA domains protect ubiquitin receptors by preventing initiation of protein degradation. *Nature Commun. 2*, 191–195.

(39) Bertolaet, B. L., Clarke, D. J., Wolff, M., Watson, M. H., Henze, N., Divita, G., and Reed, S. I. (2001) UBA domains mediate protein-protein interactions between two DNA damage inducible proteins. *J. Mol. Biol. 313*, 955–963.

(40) Kozlov, G., Peschard, P., Zimmerman, B., Lin, T., Moldoveanu, T., Mansur-Azzam, N., Gehring, K., and Park, M. (2007) Structural basis for UBA-mediated dimerization of c-Cbl ubiquitin ligase. *J. Biol. Chem. 282*, 27547–27555.

(41) Kirkin, V., McEwan, D. G., Novak, I., and Dikic, I. (2009) Role for ubiquitin in selective autophagy. *Mol. Cell 34*, 259–269.

(42) Itakura, E., and Mizushima, N. (2011) p62 targeting to the autophagosome formation site requres self-oligomerization but not LC3 binding. *J. Cell Biol. 193*, 17–27.

(43) Sims, J. J., Haririnia, A., Dickinson, B. C., Fushman, D., and Cohen, R. E. (2009) Avid interactions underlie the Lys63-linked poly-ubiquitin binding specificities observed for UBA domains. *Nat. Struct. Mol. Biol. 16*, 883–890.

(44) Albagha, O. M., Visconti, M. R., Alonso, N., Langston, A. L., Cundy, T., Dargie, R., Dunlop, M. G., Fraser, W. D., Hooper, M. J., Isaia, G., Nicholson, G. C., del Pino Montes, J., Gonzalez-Sarmiento, R., di Stefano, M., Tenesa, A., Walsh, J. P., and Ralston, S. H. (2010) Genome-wide association study identifies variants at CSF1, OPTN and TNFRSF11A as genetic risk factors for Paget's disease of bone. *Nature Genet. 42*, 520–524.

(45) Hocking, L. J., Lucas, G. J. A., Daroszewska, A., Cundy, T., Nicholson, G. C., Donath, J., Walsh, J. P., Finlayson, C., Cavey, J. R., Ciani, B., Sheppard, P. W., Searle, M. S., Layfield, R., and Ralston, S. H. (2004) Novel UBA domain mutations of SQSTM1 in Paget's disease of bone: genotype-phenotype correlation, functional analysis and structural consequences. *J. Bone Miner. Res. 19*, 1122–1127.